



RESEARCH ARTICLE

EFFECT OF MAGNESIUM DOPING ON THE STRUCTURAL STABILITY OF LAYERED LiNiO_2 BASED CATHODE MATERIALS.

N. Murali^{*1,2}, K. Ephraim Babu³, S. J. Margarette², J. M. Sailaja² and V. Veeraiiah².

1. Advanced Analytical Laboratory, DST-PURSE Programme, Andhra University
2. Department of Physics, Andhra University, Visakhapatnam, Andhra Pradesh, India
3. Department of Physics, Narasaraopeta Engineering College (A), Narasaraopet, A.P.

Manuscript Info

Manuscript History

Received: 16 August 2016
 Final Accepted: 22 September 2016
 Published: October 2016

Key words:-

Layered structure, XRD, FESEM, FT-IR.

Abstract

In rechargeable lithium batteries, nickel is employed in the form of oxide in which lithium ions are inserted into its crystal structure to form layered nickel oxide i.e., LiNiO_2 . The objective of this paper is to understand the effects of substitution of magnesium on the structural stability in the layered intercalation compounds. The compounds LiNiO_2 and $\text{LiNi}_{0.75}\text{Mg}_{0.25}\text{O}_2$ are synthesized by a solid state reaction method under the flow of air at 800°C for 24 hours. The influence of doping Mg on structure, morphology and bonding nature of cathode materials are investigated systematically. From the x-ray diffraction (XRD) data, the intensity versus diffraction angle peak indicated that the compound crystallized as a rhombohedral system (space group $R\bar{3}m$). The lattice constants and crystallite sizes were computed from XRD data. The particle morphology of the compound was observed using a field effect scanning electron microscope (FESEM). The FT-IR spectroscopic data of LiNiO_2 revealed the local structure of the oxide lattice constituted by LiO_6 and NiO_6 octahedra.

Copy Right, IJAR, 2016., All rights reserved.

Introduction:-

Over the last two decades, intensive research is going on to improve the overall performance of lithium ion batteries. The main focus has been in search of the alternative cathode materials, apart from the regular components of battery mechanisms. For the cathode materials, every system has its own advantages and disadvantages. The LiCoO_2 is a well known cathode material for rechargeable lithium ion batteries [1]. However, due to its high cost and toxicity, there has been a continuous demand during the last few years to develop alternative cathode materials which would be environmentally friendly and cost effective [2-3]. Metal based LiNiO_2 , LiMn_2O_4 and olivine type LiFePO_4 are promising materials for future to substitute LiCoO_2 . The LiNiO_2 is cheaper and less toxic compared to LiCoO_2 [4]. It delivers a larger reversible capacity with a comparable life-cycle. It is considered to be one of the best cathode materials for Lithium ion cells. The electrochemical properties of cathodes based on LiNiO_2 are good. The difficulty in synthesizing stoichiometric LiNiO_2 is also due to the loss of lithium from the host structure during high temperature calcinations because of the high vapor pressure of lithium [5-6], thus leading to the formation of non-stoichiometric structure. However, its synthesis requires special care to obtain good and reproducible performances.

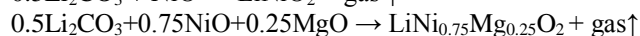
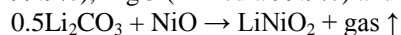
Corresponding Author:- N. Murali.

Address:- Advanced Analytical Laboratory, DST-PURSE Programme, Andhra University.

The goal of this paper is the synthesis of LiNiO_2 and $\text{LiNi}_{0.75}\text{Mg}_{0.25}\text{O}_2$ using the solid state reaction method and understanding the correlation between the structures and bonding nature.

Synthesis & Experimental Techniques:

The cathode compositions are synthesized by a solid state reaction from stoichiometric amounts of Li_2CO_3 (Himedia 99.9%), MgO (Himedia 99.9%) and NiO (Himedia 99.9%).



A slight excess amount of lithium (4%) is used to compensate for any loss of the metal which might have occurred during the calcining at high temperatures. The appropriate stoichiometric amount of the chemicals are ground in an agate mortar and calcined at 800°C for 24 h in air using a muffle box furnace.

The structural characteristics were determined by X-ray diffraction using a Rigaku Cu-K α diffractometer with diffraction angles of 10° and 80° in increments of 0.02° . The morphologies of the materials were studied by field emission scanning electron microscopy (FESEM) using Carl Zeiss, EVO MA 15, Oxford Instruments, Inca Penta FET x 3.JPG. The Fourier transform infrared spectra was recorded using Nicolet 6700 and following the KBr pressed pellet technique to determine the structures of the calcined powders.

Structure of LiNiO_2 :-

Most ABO_2 oxides are related to the rock-salt structure and are either ordered or distorted forms of NaCl (Figure 1). One possibility, exemplified by LiNiO_2 is a 1:1 ordering of the cation sites, which reduces the space group symmetry from O_h^5 (Fm3m structure) to a tetragonal D_{4h}^{19} (I41/amd structure with Z=3). The second possibility is a distortion of NaCl consisting of an elongation of the unit cell along the (111) direction; the space group is $R\bar{3}m$ with Z=1. This arrangement is sometimes known as either the NaHF_2 -type structure or the $\alpha\text{-NaFeO}_2$ -type structure. A third structure $\gamma\text{-LiAlO}_2$, which is not related to rock salt, consists of corner-linked tetrahedra in which both Li and Al are four-coordinated [7-8].

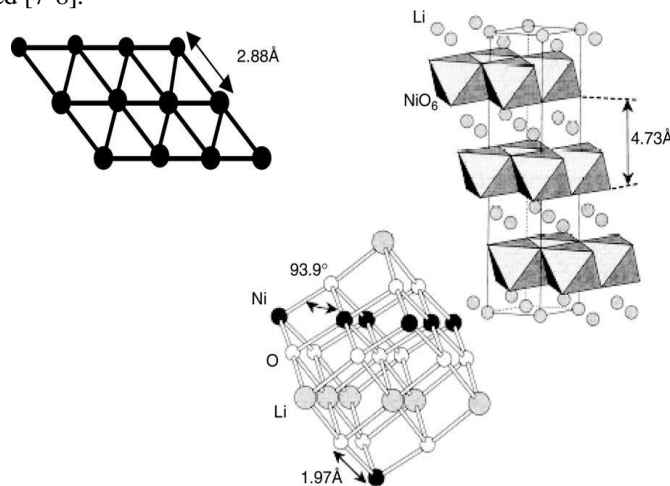


Figure 1:- Ideal structure of NaFeO_2 [8]

The layered LiMO_2 ($M = \text{Co}, \text{Mn}$ and Ni) are traditional cathode materials that have been thoroughly studied experimentally and theoretically. The layered structure can be envisioned as two interpenetrating fcc lattices, one consisting of oxygen and the other consisting of alternating (111) planes of Li and Transition Metal (TM) ions. They all belong to the $R\bar{3}m$ space group and the structure can be described as the periodic distribution of layers of MO_6 and LiO_6 octahedra stacked in an alternate manner. In the $R\bar{3}m$ space group, the Li and the metal ions remain fixed in the ideal rock salt positions, but the whole (111) oxygen planes may relax in the (111) direction giving rise to different slab spaces that affect lithium mobility. Lithium manganese oxide (LiMnO_2) has the same layered structure as LiCoO_2 and LiNiO_2 as shown in figure 2.

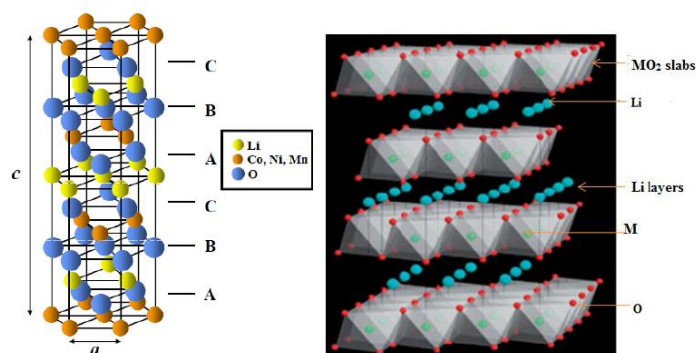


Figure 2:- The structure of layered LiMO_2 ($M = \text{Co, Mn and Ni}$) materials.

X-ray diffraction study:-

The constructive interference of X-ray radiation occurs in a material when Bragg's law is satisfied:

$$2d \sin\theta = n\lambda$$

where d is the distance between equivalent atomic planes, θ is the angle between the incident beam and these planes, n is an integer and λ is the wavelength. The scattered intensity can be measured as a function of scattering angle 2θ . Analysis of the resulting X-ray diffraction (XRD) pattern is an efficient method for determining the different phases present in the sample. Since the wavelength of X-rays used is of the same order of magnitude as the interatomic distances and bond lengths in crystalline solids ($\sim 1 \text{ \AA}$), the XRD method serves well to determine the structure of crystalline materials.

In the ideal stoichiometric LiNiO_2 (JCPDS # 090063), the Li^+ and Ni^{3+} cations are supposed to be orderly arranged along the (111) direction of the rock salt cubic lattice leading to a 2D layer structure, isostructural with $\alpha\text{-NaFeO}_2$. Hence, LiNiO_2 has a rhombohedral structure with trigonal symmetry (space group: $R\bar{3}m$) comprising of two interpenetrating close packed FCC sub-lattices: one consists of oxygen anions, and the other consists of Li and Ni cations on alternating (111) planes [8].

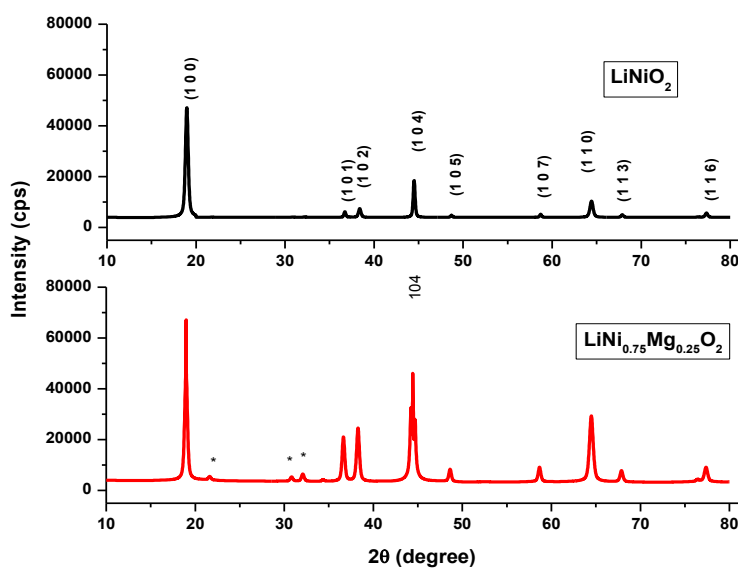


Figure 3:- XRD spectra for LiNiO_2 and $\text{LiNi}_{0.75}\text{Mg}_{0.25}\text{O}_2$

Figure 3 shows the XRD patterns of $\text{LiNi}_{0.75}\text{Mg}_{0.25}\text{O}_2$. It can be seen from the patterns that all diffraction peaks are very strong, which indicate that the samples have good crystal structure. The diffraction peaks are closely matched

with those of LiNiO_2 . No impurities were observed in the XRD patterns. This indicates that the element Mg is well substituted for Ni in $\text{LiNi}_{0.75}\text{Mg}_{0.25}\text{O}_2$. Hence, it is thought that the solid state reaction process is quite effective to synthesize multi element-containing oxides and carbonates [9-10].

Table 1:- Lattice constants (a, c) and c/a ratio for LiNiO_2 and $\text{LiNi}_{0.75}\text{Mg}_{0.25}\text{O}_2$

Material	a Å	c Å	c/a	Crystallite size (nm)	Space group
LiNiO_2	2.581	14.918	5.779	42.96	rhombohedral ($R\bar{3}m$)
$\text{LiNi}_{0.75}\text{Mg}_{0.25}\text{O}_2$	2.501	14.930	5.969	40.21	rhombohedral ($R\bar{3}m$)

we calculated the crystallite size at different orientations for these materials from their line width in the XRD pattern by using Debye-Scherrer's formula: $D=0.9\lambda/\beta\cos\theta$, where λ is the wavelength of the X-ray used (1.54 Å), β is the full width half maximum in radians, θ is Bragg's angle. In short, the crystal structure of the material cannot be changed by Magnesium doping. However, the crystal parameters were influenced. The calculated lattice parameters a, c, c/a and unit-cell volume are summarized in Table 1.

Field Effect Scanning Electron Microscope Observations:-

The field effect scanning electron microscope (FESEM) is used to study the surface morphology of the sample. It is an electron microscope and it takes the images of the surface of the samples by scanning it with a high energy beam of electrons. The FESEM can produce very high-resolution images of the sample surface, revealing details of the order less than 1 nm in size. This also produce images of high resolution, which means that closely spaced features can be examined at high magnification.

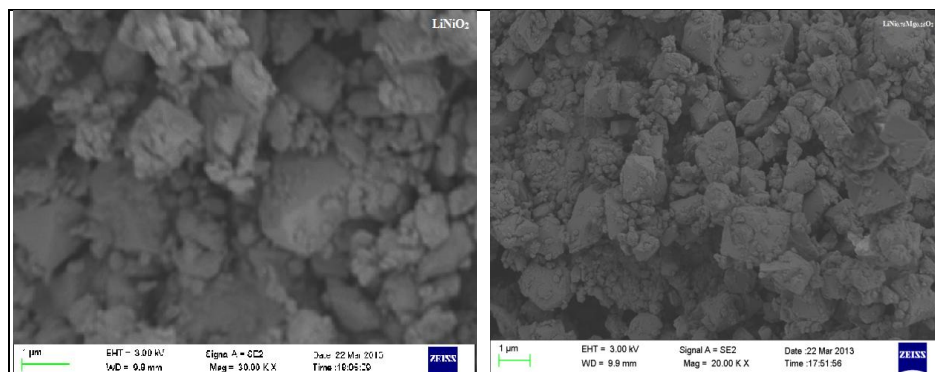


Figure 4:- FESEM images for LiNiO_2 and $\text{LiNi}_{0.75}\text{Mg}_{0.25}\text{O}_2$

The field effect scanning electron micrographs of LiNiO_2 and $\text{LiNi}_{0.75}\text{Mg}_{0.25}\text{O}_2$ calcined sample at 800°C for 24 h in air are presented in Figure 4. The powder of pure LiNiO_2 consists of quite small particles of uniform size. The powders calcined for both the compounds comprised of particles of similar shape and size. The particles are generally in the form of smooth-edged polyhedra and their average size is approximately 1.5 - 2 μm . This unique morphology is advantageous for electrode materials, because it allows the electrochemical performance to be improved.

Fourier Transform Infrared spectra observations:-

Typical FT-IR spectra of LiNiO_2 and $\text{LiNi}_{0.75}\text{Mg}_{0.25}\text{O}_2$ materials synthesized by solid state reaction method are depicted in Figure 5. The FT-IR spectra of the powders displayed the predominance of the stretching modes and the IR resonant frequency of LiO_6 octahedra located between 400 and 460 cm^{-1} . There are four infrared active vibrations such as $2A_{2u}+2E_u$ for the D_{3d}^5 group based on group theory analysis [11]. The Wyckoff sites 3(a) and 3(b) consist of transition metal cations (i.e., Ni, Mg) and lithium ions respectively. The $\text{LiNi}_{0.75}\text{Mg}_{0.25}\text{O}_2$ materials are separated into LiO_2 and MgO_2 layers which can be identified in the range of 400-600 cm^{-1} . The band observed around 500 cm^{-1} may be assigned to the asymmetric stretching modes of Mg-O bonds in MgO_6 octahedra and the other band around 550 cm^{-1} may be attributed to the O-Mg-O bending modes [12]. The broadening of FT-IR bands is due to the cation mixing in the crystal layers. When Magnesium substitution increases, the stretching and bending mode frequencies slightly shift to higher wavenumber regions, which may be attributed to a change in Mg-O covalency [13].

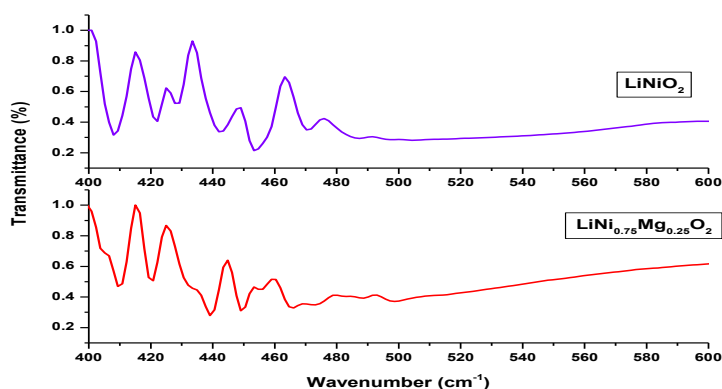


Figure 5:- FTIR spectra for LiNiO_2 and $\text{LiNi}_{0.75}\text{Mg}_{0.25}\text{O}_2$

The frequency shift of both the stretching and bending modes as a function of the magnesium doping leads to the cationic disorder in the $(\text{Ni}_{0.75}\text{Mg}_{0.25})\text{O}_2$ slabs. The frequency shift of the LiO_6 mode has two origins:

1. The slight expansion of the interslab distance (c_{hex} cell parameter) with increasing temperature.
2. The small mixing of Li-O stretching and O-Ni-O bending motion present in the low-wavenumber peak.

Figure 5 shows the variation of the frequencies of the high-wavenumber IR-modes with the Co content in $\text{Ni}_{0.75}\text{Mg}_{0.25}\text{O}_2$ oxides. [14].

Conclusions:-

By adopting solid state reaction method, we could successfully synthesize the two compounds LiNiO_2 and $\text{LiNi}_{0.75}\text{Mg}_{0.25}\text{O}_2$ in the present study. Using this method, the particles were successfully obtained with homogeneous distribution. X-ray diffraction patterns confirmed that the synthesized materials have a well developed layered $\alpha\text{-NaFeO}_2$ structure. The material with Mg stoichiometry had better hexagonal ordering compared to the LiNiO_2 and the FT-IR results confirmed the presence of M-O bonds in MO_6 octahedra. The FESEM images showed that the agglomerations are of well crystalline submicron particles of size 1.5-2 μm . The powders of pure LiNiO_2 and $\text{LiNi}_{0.75}\text{Mg}_{0.25}\text{O}_2$ consisted of quite small particles of uniform size.

Acknowledgement:-

The authors (N. Murali and S. J. Margarette) gratefully acknowledge the financial support of University Grants Commission, New Delhi, India through UGC-SAP and MAMS fellowships respectively for this research work.

References:-

1. Y. Makimura, T. Ohzuku, Journal of Power Sources, 119-121 (2003) 156-160.
2. M. Broussely, F. Pertont, P. Biensan, J.M. Bodet, J. Labat, A. Lecerf, C. Delmas, A. Rougier, J.P. Peres, Journal of Power Sources, 54 (1995) 109-114.
3. P. Kalyani, N. Kalaiselvi, N. Muniyandi, J. Power Sources 111 (2002) 232-238.
4. Y. Makimura, T. Ohzuku, Journal of Power Sources, 119-121 (2003) 156-160.
5. M. Broussely, F. Pertont, P. Biensan, J.M. Bodet, J. Labat, A. Lecerf, C. Delmas, A. Rougier, J.P. Peres, Journal of Power Sources, 54 (1995) 109-114.
6. P. Periasamy, N. Kalaiselvi, R. Thirunakaran, T. Premkumar, N.G. Renganathan, M. Raghavan, N. Muniyandi, Int. J. Inorg. Mater. 3 (2001) 401-407.
7. J.R. Dahn, V. von Sacken, C.A. Michal, Solid State Ionics 44 (1990) 87.
8. P. Kalyani, N. Kalaiselvi, Science and Technology of Advanced Materials 6 (2005) 689-703
9. H. Tukamoto and A. R. West, J. Electrochem. Soc. 144, 3164 (1997)
10. Y. I. Jang, B. Huang, H. Wang, D. R. Sadoway, G. Ceder, Y. M. Chiang, H. Liu, and H. Tamura, J. Electrochem. Soc. 146, 862 (1999).
11. D. Linden, Handbook of Batteries, Mc Graw Hill Book Co, NY, 1984, p. 2.3.
12. A. Rougier, G. A. Nazri, C. Julien, Ionics 3 (1997) 170.
13. C. Julien, M. Massot, Phys. Chem. Chem. Phys. 4 (2002) 4226.
14. C. Julien, C. Letranchant, S. Rangan, M. Lemal, S. Ziolkiewicz, S. Castro-Garcia, L. El-Farh, M. Benkaddour, Mater. Sci. Eng. B 76 (2000) 145.